Transport properties, thermodynamic properties, and electronic structure of $SrRuO_3$

P. B. Allen*
Institut Romand de Recherche Numérique en Physique des Materiaux (IRRMA), IN-Ecublens, CH-1015 Lausanne, Switzerland and Departement de Physique de la Matière Condensée, Université de Genève, 24 Quai Ernest-Ansermet, CH-1211 Geneva 4, Switzerland

H. Berger, O. Chauvet, and L. Forro
École Polytechnique Federale de Lausanne, Departement de Physique, CH-1015 Lausanne, Switzerland

T. Jarlborg, A. Junod, B. Revaz, and G. Santi
Departement de Physique de la Matière Condensée, Université de Genève, 24 Quai Ernest-Ansermet, CH-1211 Geneva 4, Switzerland
(Received 22 August 1995)

$SrRuO_3$ is a metallic ferromagnet. Its electrical resistivity is reported for temperatures up to 1000 K, its Hall coefficient for temperatures up to 300 K, and its specific heat for temperatures up to 230 K. The energy bands have been calculated by self-consistent spin-density functional theory, which finds a ferromagnetic ordered moment of $1.45\mu_B$ per Ru atom. The measured linear specific heat coefficient γ is 30 mJ/mol, which exceeds the theoretical value by a factor of 3.7. A transport mean free path at room temperature of ≈ 10 Å is found. The resistivity increases nearly linearly with temperature to 1000 K in spite of such a short mean free path that resistivity saturation would be expected. The Hall coefficient is small and positive above the Curie temperature, and exhibits both a low-field and a high-field anomalous behavior below the Curie temperature.

I. INTRODUCTION

$SrRuO_3$ has a nearly cubic perovskite structure.[1,2] The combination of good chemical stability, good metallic conductivity,[3] and easy epitaxial growth on various perovskite substrates[4–6] makes it attractive for possible multilayer device applications.[7] There is some evidence[8] that above ≈ 800 K the structure reverts to cubic. Nominally single crystals are therefore likely to be randomly twinned arrangements of the three orientations of orthorhombic ordering. Below $T_c = 160$ K it is ferromagnetic with a moment $1.1\mu_B$ at $T = 0$ K,[9] the largest ordered moment known to arise from $4d$ electrons. Assuming a nominal valence Ru^{4+} and configuration $4d(t_{2g})^4$, full Hund's rule spin alignment ($\uparrow t_{2g}^3$, $\downarrow t_{2g}^1$) predicts a moment $2\mu_B$ and insulating ("half-metallic") behavior of the majority spins. The deficiency of moment has received three explanations, (1) collective (rather than atomic) band magnetism,[10] (2) spin canting,[11] and (3) incomplete alignment of magnetization in different domains due to large magnetocrystalline anisotropy and random crystallographic domain alignment.[12] In this paper we offer transport and thermodynamic data, and a band structure calculation which agrees with the band magnetism view of the reduced moment. In particular, the specific heat shows a very large Fermi level density of states, which band theory assigns to both majority and minority spins, with majority spins slightly more numerous. The majority spin electrons have a small Fermi velocity, suggesting that most of the transport currents are carried by minority spin electrons.

II. ELECTRONIC STRUCTURE

The electronic structure calculations were done using the self-consistent linear muffin-tin orbital (LMTO) method[13] in the local spin-density approximation (LSDA). The calculations for the distorted unit cell, containing 20 atoms, were converged using 64 k points in the irreducible (1/8) Brillouin zone. The density of states (DOS) and Fermi velocities were calculated by tetrahedron integration using a finer k-point mesh. The structural parameters were taken from Ref. 14.

A first calculation was done for the undistorted cubic structure with five atoms per cell. The shape of the DOS is similar to that for the real unit cell, except for details. The DOS value per atom at the Fermi energy (E_F) is somewhat smaller than for the large cell, making the Stoner factor (1.04) and magnetic moment ($0.6\mu_B$) smaller. The total energy is lower by about 25 mRy per formula unit (f.u.) in the ferromagnetic configuration compared to the paramagnetic case. For the remaining discussion we give only the results from the calculations for the large distorted cell.

Figure 1 shows the DOS for the two spins. The bands extending from about -8 eV to about -3 eV relative to E_F are primarily of oxygen p parentage. There is a gap of about 1 eV separating these from bands of primarily (74%) Ru d parentage. The Fermi level lies about 2 eV above the bottom of these bands, filling to about two-thirds occupancy a region of high density of states, presumably associated with the t_{2g} orbitals which are mixed mostly through π overlap with oxygen p states. The positions of these levels accord well with the assignments made by Cox *et al.*[15] based on ultraviolet photoemission spectroscopy (UPS) measurements. Above the Fermi level comes an increasing amount of Ru s and Sr s and d levels in addition to the Ru d states of e_g character. In the paramagnetic case when the exchange splitting is zero, E_F falls near the peak in the DOS so that the Stoner factor becomes quite large, 1.39. Thus a ferromagnetic transition is expected, mainly due to the Ru d band, and the magnetic moment is $1.45\mu_B$ per Ru atom in the spin

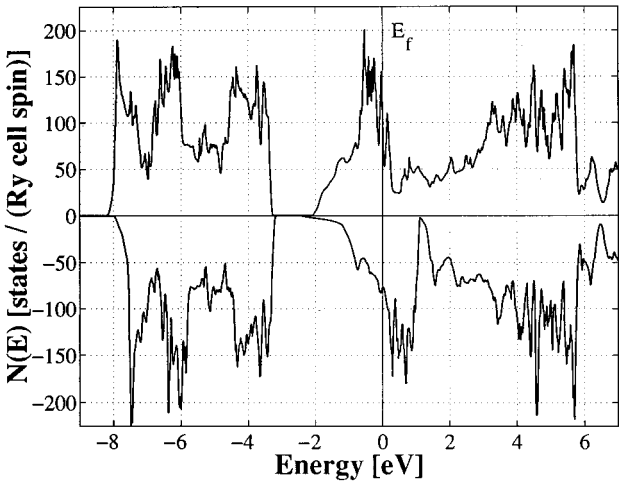

FIG. 1. Electronic density of states of ferromagnetic $SrRuO_3$. Majority spin is plotted upward, minority spin downward. The cell contains four formula units.

polarized calculation. The other atoms have only small moments, about $0.06\mu_B$ and $0.14\mu_B$ per Sr and O atom, respectively. The total energy difference between the ferromagnetic and paramagnetic configuration is about 24 mRy per f.u. Our calculated moment exceeds the zero-field measured value $\approx 1.1\mu_B$.[9] There is some uncertainty in the true value of the saturation magnetization. Kanbayasi[12] extrapolates a high-field value as great as $2\mu_B$. It is possible that a large magnetocrystalline anisotropy[9,12,16] pins the magnetization perpendicular to the orthorhombic c axis of the distorted structure, which is randomly aligned in the nominally single-crystal sample.

It is interesting that our calculated moment is so sensitive to the small distortion of crystal structure from cubic. This accords with the discovery by Kirillov *et al.*[17] that optic phonon modes are affected by the magnetic order.

Table I shows the calculated value of the density of states at the Fermi surface for each atom species and spin type, and also the calculated values of the Fermi velocity and Fermi surface area. Three bands of majority spins cross the Fermi level, with quite small Fermi velocities, whereas eight bands of minority spin cross the Fermi level with more ordinary size Fermi velocities. The DOS at E_F, $N(E_F)$, is sensitive to changes in the magnetic moment, because of the position of E_F on the downslope of majority and upslope on the minority spins as shown in Fig. 1. At convergence we find the total $N(E_F)=$ 190 states/(Ry cell), where 60% is majority spin. This DOS is concentrated on the Ru sites, making the value very high per Ru atom. The DOS is even higher in the paramagnetic state, where the Fermi surface lies in a region of very small Fermi velocity. Ferromagnetic ordering diminishes the area of the Fermi surface to 75% of the paramagnetic state value, mostly by diminishing the area of the up spin surface. The DOS is reduced to 58% of the paramagnetic value. The up spin contribution is diminished because of the reduced area of Fermi surface, and the down spin contribution is reduced because of the increased Fermi velocity.

Recently we learned of an unpublished linearized augmented-plane-wave (LAPW) calculation by Singh.[18] Near the Fermi level, Singh's results agree very closely with ours, including the size of the ordered moment. Farther away there are interesting differences of detail, but reasonable qualitative accord.

III. SPECIFIC HEAT

Polycrystalline samples of mass ≈0.5 g were prepared for specific heat measurements. Stoichiometric mixtures of SrO_2 and RuO_2 (99.9% Atomergic Chemetals) were first heated for 24 h at 1000 °C and refired again for 80 h at 1100 °C. Several grindings were done in an agate mortar between the thermal treatments in order to get homogeneous samples. After 50 h at 1150 °C the reactions were fully realized, and slow quenching (10 °C/h) was done under oxygen. X-ray powder diffraction of this product showed a single phase consistent with the previous report of Jones *et al.*[2]

The low temperature heat capacity measurement used a thermal relaxation technique with 1% accuracy.[19] The polycrystalline sample, 47 mg in mass, was measured in zero external field between 1.2 and 32 K. Figure 2 shows the data below 7 K in the usual C/T vs T^2 plot. Below 10 K the data are fit by the low T approximation

$$\frac{C}{T}=\gamma+\frac{12}{5}R\pi^4\frac{T^2}{\Theta_D^3}, \tag{1}$$

where γ is the Sommerfeld constant and Θ_D the Debye temperature in the limit $T\to 0$. From a least squares fit between 1 and 7 K we extract the values $\gamma=6.0$ mJ/atg (1 atg is 47.3 g or 1/5 mol $SrRuO_3$) and $\Theta_D=368$ K. Deviations occur at higher temperature, indicating that Θ_D has a minimum near 25 K and then increases with T. Such a variation is quite common and reflects additional modes in the 10 meV range beyond those in the Debye distribution. The measured γ corresponds to a Fermi level DOS of 173 states/(Ry f.u.) (both spins) which exceeds the band theoretical value by a factor $1+\lambda_\gamma\equiv\gamma_{\rm expt}/\gamma_{\rm theor}=3.7$. Almost an identical enhancement

TABLE I. Calculated properties of $SrRuO_3$.

		DOS [states/(Ry cell)]				$\langle v_{F,x}^2\rangle$	$\langle v_{F,y}^2\rangle$	$\langle v_{F,z}^2\rangle$	Area of FS
		Sr	Ru	O_3	Total		[10^{14} cm^2/s^2]		[10^{17} cm^{-2}]
Paramagnetic		12	246	67	325	0.6	0.8	0.7	1.06
Magnetic	Up	5	84	25	114	1	0.6	0.6	0.68
	Down	4	55	17	76	3.5	2.6	2.0	0.91
	Total	9	139	42	190	2.0	1.4	1.2	1.59

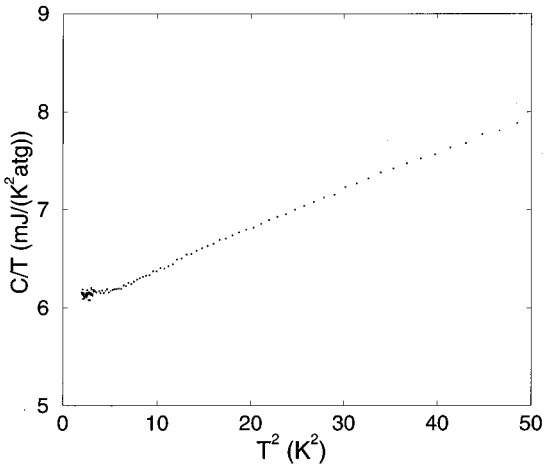

FIG. 2. Low temperature specific heat C/T plotted versus T^2 for $SrRuO_3$.

of experiment over theory was recently found for the layered metal Sr_2RuO_4.[20,21] By contrast, the rutile structure metal RuO_2 has a theoretical density of states at the Fermi surface which is only half as large per ruthenium atom.[22] Comparing with the measured specific heat[23] this corresponds to a value $\lambda_\gamma = 0.45$, close to what is expected from normal electron-phonon mass enhancement. Thus RuO_2 appears to be a conventional metal, while both $SrRuO_3$ and Sr_2RuO_4 have large mass enhancements λ_γ presumably caused less by electron-phonon effects than by spin fluctuations or some other kind of Coulomb correlation effect.

Figure 3 shows the high temperature specific heat of a 0.36 g sample cut from the same ceramic mass, and measured in an adiabatic, continuous heating calorimeter.[24] The accuracy is 1% and the scatter 0.02%. The full width of the ferromagnetic transition exceeds the temperature steps used in data reduction by about two orders of magnitude.

The total specific heat approaches 20 J/(atg K) at $T = 250$ K, a relatively low value compared to the Dulong-Petit saturation at 24.94 J/(atg K). Neglecting electronic contributions, this sets a lower limit to the Debye temperature,

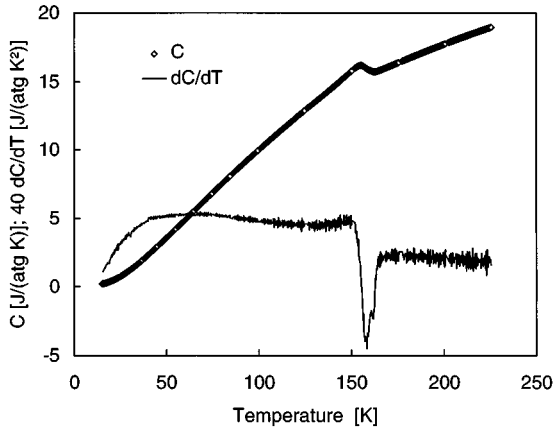

FIG. 3. Specific heat $C(T)$ (diamonds) and derivative $dC(T)/dT$ (full line; note the scale factor) for $SrRuO_3$ in the 15–250 K range.

$\Theta_D(250\ \mathrm{K}) > 540$ K, significantly higher than the low temperature value, 368 K. This comparison suggests that the phonon density of states is widely dispersed, including high frequency optical modes from ruthenium-oxygen bond stretching vibrations.

The ferromagnetic transition centered at $T_c \approx 160$ K appears as a surprisingly small step rather than the quasilogarithmic divergence frequently seen. A closer look at the derivative of the specific heat in Fig. 3 shows two transition components at 158 and 162 K, perhaps caused by sample inhomogeneity. No significant anomaly is seen in the range 35–45 K where the resistivity shows some structure (see below).

The entropy associated with the transition can be estimated by subtracting phonon and spinless electronic contributions to the specific heat. Most of the magnetic entropy in model systems with well-localized spins is released in a specific heat peak extending from $\approx 0.5T_c$ to $\approx 1.5T_c$, i.e., from 80 to 240 K, and should equal $R\ln 3$ or $R\ln 2$ for full disordering of localized spin 1 or 1/2 ions which are fully ordered at $T = 0$. Since we have no clear way to make this subtraction, we used two different methods, modeled after a critical transition and a mean-field transition respectively. Phonons were modeled by sums of Einstein functions and electrons were assumed to give a contribution γT. The results for the integrated entropy ΔS in the interval 40–200 K were ≈ 1.1 J/(atg K) and 2.7 J/(atg K), respectively, by the two methods. These correspond to 12% and 30% of $R\ln 3$. Apparently no more than 1/3 of the entropy of $S = 1$ Ru spins is removed by ferromagnetic ordering. However, if we assume an electronic term γT with γ independent of temperature and having the value measured at low T, as was done in both entropy estimates, then there is a lot of electronic entropy ($\approx 0.7R$ per Ru atom) removed by cooling from 200 K to $T = 0$. It is probably not correct to attempt a complete separation between electronic and magnetic entropy.

IV. TRANSPORT PROPERTIES

Single-crystal samples of dimensions $\approx 1 \times 1 \times 0.5$ mm were grown for resistivity measurements by slow cooling in $SrCl_2$ flux.[25] First polycrystalline $SrRuO_3$ was prepared from stoichiometric quantities of RuO_2 (99.9%) and $SrCO_3$ (99.99%). The single-phase product was mixed with $SrCl_2$ anhydrous in the weight ratio 1:30, and placed in a 50 cm^3 platinum crucible covered with a platinum lid in a vertical furnace with programmable temperature control. The refractory crucible supports induced a small temperature gradient towards the base of the crucible. The flux mixture was heated to 1260 °C (200 °C/h) for homogenization of the melt, soaked for 40 h, and cooled to 800 °C (at 2 °C/h). The crucibles were then removed and cooled quickly to room temperature. Crystals a few mm in size were easily separated from the frozen flux by immersing the crucible in hot water.

Resistivity was measured in a four-probe configuration on samples of typical dimensions $\approx 1 \times 0.5 \times 0.05$ mm^3. Approximately ten samples were measured. The major features were reproducible, i.e., the break in slope at T_c, the qualitative shape, and the absolute magnitude (to within a factor of 2). We attempted to measure the anisotropy of resistivity between the long axis and the thin axis of the samples; the

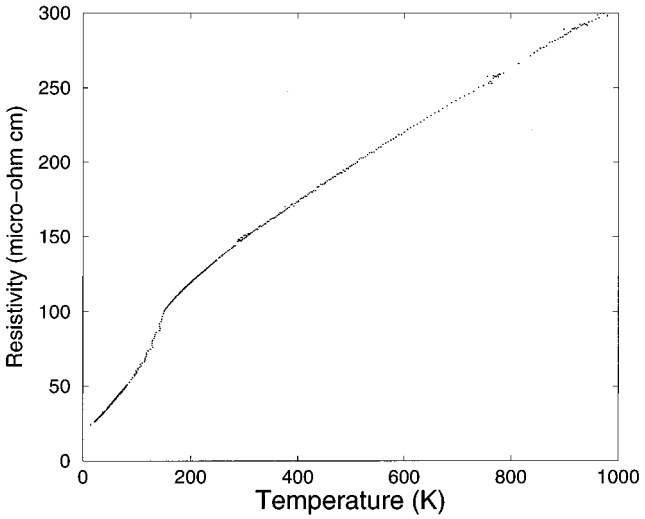

FIG. 4. Resistivity versus temperature for $SrRuO_3$.

effect was less than 10%. Given that LSDA band theory (Sec. II) finds an orthorhombic anisotropy varying from 10% to 40%, the lack of measurable anisotropy of our samples may mean that there is a random distribution of orthorhombic domains or twins in our samples. Results for one of our samples up to 1000 K are shown in Fig. 4.

The electrical resistivity has been reported previously at temperatures below 300 K. Polycrystalline samples were reported in Refs. 3, 14, and 26, single crystals in Ref. 25, and oriented thin film samples in Refs. 5–7. Our data agree with all measurements concerning the shape of $\rho(T)$ and the break in slope at $T_c \approx 160$ K. Measurements on polycrystalline samples tend to yield absolute magnitudes of $\rho(T)$ about five times larger than seen on single-crystal or oriented film samples. Our measurements, as well as previous ones on single crystals or oriented films, show a surprising sample dependence in the low temperature power law, with the exponent p [defined by $\rho(T)-\rho(0) \propto T^p$] appearing to vary between 1 and 2.

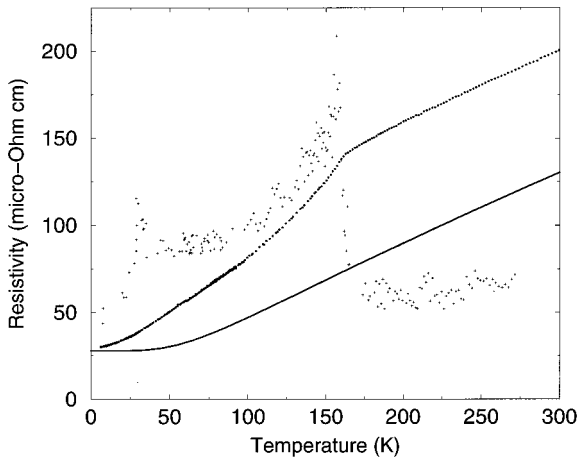

FIG. 5. Resistivity versus temperature for $SrRuO_3$ from 0 to 300 K, with a Bloch-Grüneisen curve (solid line) for comparison, and $d\rho/dT$ in arbitrary units.

Figure 5 shows the resistivity on a different sample in the range 0–300 K, along with the derivative $d\rho/dT$ and a Bloch-Grüneisen curve. As is typical in metallic ferromagnets, there is a peak in $d\rho/dT$ at the Curie point, similar to the peak in $C(T)$. We presume that the resistivity can be composed of a sum of electron-phonon scattering and spin-fluctuation scattering. Above the Curie temperature, the spin-fluctuation part should slowly saturate at an approximately temperature-independent value. The Bloch-Grüneisen curve in Fig. 5 is chosen to match the slope of the data at high temperature. Insofar as this curve represents a fair estimate of the electron-phonon contribution to $\rho(T)$, we can use it[27] to extract a value of the electron-phonon coupling constant λ_{tr}. Lacking more detailed information, we assume that the scattering rate is the same for up and down spin electrons, and roughly constant for all electrons at the Fermi surface. Then $\sigma=\Omega_p^2\tau/4\pi$ where the Drude plasma frequency Ω_p^2 is defined by

$$\Omega_{xx}^2=\frac{4\pi e^2}{\Omega_{\rm cell}}\sum_{k\sigma} v_{k\sigma x}^2\delta(\epsilon_{k\sigma}-\epsilon_F). \tag{2}$$

From the values given in Table I, the xx, yy, and zz components of the Drude plasma frequency tensor have the values 3.0, 2.5, and 2.3 eV in the ferromagnetic state, and 2.2, 2.5, and 2.3 eV in the paramagnetic state. For a random mixture of orthorhombic domains we should use the root mean square value, $\Omega_p=2.6$ eV (ferromagnetic) or 2.3 eV (paramagnetic). Using a Debye spectrum with $\Theta_D=368$ K, the curve of Fig. 5 corresponds to $\lambda_{tr}=0.5$, calculated using the paramagnetic state value of the Drude plasma frequency. This is similar to the value found in Ref. 22 for RuO_2. However, because LSDA band theory agrees well with the specific heat γ in the latter compound but not in $SrRuO_3$, the value of λ_{tr} found here cannot be regarded as particularly reliable.

It is surprising how rapidly thermal scattering sets in as temperature increases from $T=0$, much more rapidly than the Bloch T^5 law, but sample dependent as mentioned above. We do not understand the origin of either the rapid rise of $\rho(T)$ or its sample dependence. Independent of a model for the scattering, however, we can estimate the carrier mean free path ℓ, using the equation[27]

$$\sigma=\frac{e^2}{24\pi^3\hbar}[A_{\rm FS\uparrow}\ell_\uparrow+A_{\rm FS\downarrow}\ell\downarrow], \tag{3}$$

where $A_{\rm FS}$ is the Fermi surface area. This result depends only on the assumption of not having too strong a variation of ℓ_k from point to point on the Fermi surface. For paramagnetic materials with $A_{\rm FS\uparrow}=A_{\rm FS\downarrow}$, Eq. (3) permits a robust estimate of the average mean free path, since local-density approximation (LDA) band theory generally gets the shape of the Fermi surface to very good accuracy, not contaminated by renormalization or other likely errors of LDA. In the ferromagnetic case, we are less certain about the correctness of LSD theory concerning spin splitting; therefore the separate values of $A_{\rm FS\uparrow}$ and $A_{\rm FS\downarrow}$ are less robust. Using the room temperature resistivity of 200 $\mu\Omega$ cm for the sample shown in Fig. 5, and the paramagnetic value of the Fermi surface area, the room temperature mean free path is 7 Å, as small as

is found in good superconductors with the A15 (Cr_3Si) structure. However, unlike the case of A15 superconductors, there is no sign of ''saturation'' of the resistivity [$\rho(T)$ approaching a temperature-independent value]. If the value $\rho(300\ \mathrm{K}) = 150\ \mu\Omega$ cm from Fig. 4 is used, ℓ becomes ≈ 10 Å. This is still short enough that the Boltzmann quasiparticle gas theory should not be applicable.[27]

The origin of this short room temperature mean free path is the small Fermi velocity found by LDA band theory in the paramagnetic phase. One way of having a larger mean free path is to argue that the paramagnetic state has fluctuating spins with medium range order, so that locally for time intervals not too long the energy bands are really the ferromagnetic bands. The areas of the up and down spin Fermi surfaces are not very different. However, assuming a roughly constant time between scattering events, the small velocity of the majority spin carriers suggests a significantly smaller mean free path for the up spins than for the down spins. Therefore we assume that the second term of Eq. (3) dominates, and find from the data of Fig. 5 an upper limit $\ell_{\downarrow}(300\ \mathrm{K}) = 17$ Å, or 22 Å using the data of Fig. 4. The up spin electrons are unlikely to have a mean free path larger than ≈ 9 Å. By $T = 500$ K, even the down spin electrons should have $\ell < 10$ Å, and Boltzmann theory should fail visibly. However, the resistivity as shown in Fig. 4 continues to rise almost linearly for T up to 1000 K. The origin of this behavior is not known, but is reminiscent of the resistivity seen in high T_c superconductors and seen also in the high T metallic phase of VO_2.[28]

Our samples show a small but significant enhancement in $d\rho/dT$ in the range 35–45 K (Fig. 5). This effect is sample dependent. In exactly this range, Kanbayasi[29] found a dramatic change in magnetocrystalline anisotropy and presumed change in orientation of the magnetization in certain samples called ''tetragonal'' rather than ''pseudocubic'' (orthorhombic). However, no sign of anomaly can be seen in the specific heat measured on polycrystalline samples in this range (Fig. 3). Possibly our nominally single-crystal samples actually contain varying amounts of Kanbayasi's second crystal structure.

The Hall effect was measured in a six-probe configuration, with a typical current of 10 mA and magnetic field up to 12 T. The sign of the Hall voltage was calibrated with a sample of $Bi_2Sr_2CaCu_2O_8$ superconductor. Figure 6 shows typical curves of Hall voltage versus field at temperatures above and below the Curie temperature. Above T_c at 190 K there is a normal weak positive Hall coefficient,

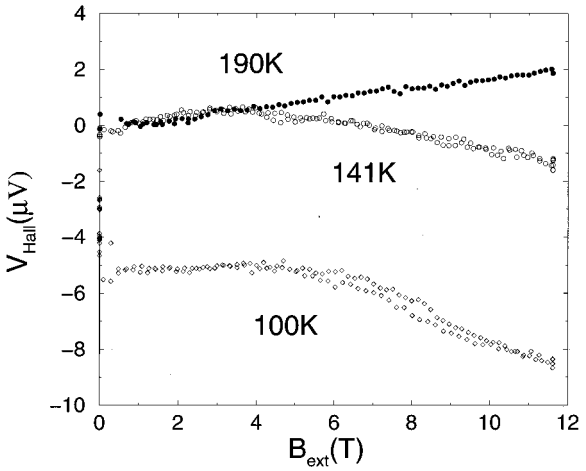

FIG. 6. Hall voltage versus field for $SrRuO_3$ at three temperatures.

$\approx 2\times 10^{-10}\ \mathrm{m}^3/\mathrm{C}$, which diminishes gradually at higher T. Just below T_c at 140 K, the data could be interpreted as showing the sum of an anomalous Hall effect of positive sign and an ordinary Hall effect of negative sign. However, the crossover field (≈ 4 T) is much too large. The data at 100 K show clearly that there are three regimes of field, with an anomalous Hall effect occurring in very weak fields, not resolved in our experiment, and then two higher-field regimes, each characterized by approximately linear behavior of V_H with applied field, but with a slope change near 6 T.

Since the Fermi surface contains both holelike and electronlike regions, it is very difficult to predict from the band structure how R_H should behave. The temperature variation can be rationalized in a model where electron-phonon scattering is dominant on the holelike parts and spin-fluctuation scattering dominates on electronlike parts. As temperature increases for $T > T_c$, electron-phonon scattering increases while spin-fluctuation scattering saturates. This drives conductivity increasingly onto the electronlike parts of Fermi surface.

ACKNOWLEDGMENTS

We thank C. H. Ahn, P. Almeras, L. Miéville, J.-M. Triscone, Z.-G. Ye, and K. Yvon for helpful discussions. P.B.A. was supported in part by U. S. NSF Grant No. DMR-9417755.

*Permanent address: Dept. of Physics, SUNY Stony Brook, Stony Brook, NY 11794-3800.

[1] A. Callaghan, C. W. Moeller, and R. Ward, Inorg. Chem. **5**, 1572 (1966).

[2] C. W. Jones, P. D. Battle, P. Lightfoot, and W. T. A. Harrison, Acta Crystallogr. Sect. C **45**, 365 (1989).

[3] Y. Noro and S. Miyahara, J. Phys. Soc. Jpn. **27**, 518 (1969).

[4] C. B. Eom, R. J. Cava, R. M. Fleming, J. M. Phillips, R. B. van Dover, J. H. Marshall, J. W. P. Hsu, J. J. Krajewski, and W. F. Peck, Jr., Science **258**, 1766 (1992).

[5] C. B. Eom, R. B. Van Dover, J. M. Phillips, D. J. Werder, J. H. Marshall, C. H. Chen, R. J. Cava, R. M. Fleming, and D. K. Fork, Appl. Phys. Lett. **63**, 2570 (1993).

[6] X. D. Wu, S. R. Foltyn, R. C. Dye, Y. Coulter, and R. E. Muenchhausen, Appl. Phys. Lett. **62**, 2434 (1993).

[7] L. Antognazza, K. Char, T. H. Geballe, L. L. H. King, and A. W. Sleight, Appl. Phys. Lett. **63**, 7 (1993).

[8] G. L. Catchen, T. M. Rearick, and D. G. Schlom, Phys. Rev. B **49**, 318 (1994).

[9] A. Kanbayasi, J. Phys. Soc. Jpn. **41**, 1876 (1976).

[10] J. M. Longo, P. M. Raccah, and J. B. Goodenough, J. Appl. Phys. **39**, 1327 (1968).

[11] T. C. Gibb, R. Greatrex, N. N. Greenwood, D. C. Puxley, and K. G. Snowdon, J. Solid State Chem. **11**, 17 (1974).

[12] A. Kanbayasi, J. Phys. Soc. Jpn. **44**, 89 (1978).
[13] O. K Andersen, Phys. Rev. B **12**, 3060 (1975); T. Jarlborg and G. Arbman, J. Phys. F **7** 1635 (1977).
[14] M. Shikano, T. K. Huang, Y. Inaguma, M. Itoh, and T. Nakamura, Solid State Commun. **90**, 115 (1994).
[15] P. A. Cox, R. G. Egdell, J. B. Goodenough, A. Hamnett, and C. C. Naish, J. Phys. C **16**, 6221 (1983).
[16] L. Klein, J. S. Dodge, T. H. Geballe, A. Kapitulnik, A. F. Marshall, L. Antognazza, and K. Char, Appl. Phys. Lett. **66**, 2427 (1995).
[17] D. Kirillov, Y. Suzuki, L. Antognazza, K. Char, I. Bozovic, and T. H. Geballe, Phys. Rev. B **51**, 12825 (1995).
[18] D. J. Singh, J. Appl. Phys. (to be published).
[19] D. Sanchez, A. Junod, J.-Y. Genoud, T. Graf, and J. Muller, Physica C **200**, 1 (1992).
[20] Y. Maeno, H. Hashimoto, K. Yoshida, S. Nishizaki, T. Fujita, J. G. Bednorz, and F. Lichtenberg, Nature (London) **372**, 532 (1994).
[21] T. Oguchi, Phys. Rev. B **51**, 1385 (1995); D. J. Singh, *ibid.* **52**, 1358 (1995).
[22] K. M. Glassford and J. R. Chelikowsky, Phys. Rev. B **49**, 7107 (1994); J. H. Xu, T. Jarlborg, and A. J. Freeman, *ibid.* **40**, 7939 (1989).
[23] B. C. Passenheim and D. C. McCollum, J. Chem. Phys. **51**, 320 (1969).
[24] A. Junod, E. Bonjour, R. Calemzuk, J.-Y. Henry, J. Muller, G. Triscone, and J. C. Vallier, Physica C **211**, 304 (1993).
[25] R. J. Bouchard and J. L. Gillson, Mater. Res. Bull. **7**, 873 (1972).
[26] J. J. Neumeier, A. L. Cornelius, and J. S. Schilling, Physica B **198**, 324 (1994).
[27] P. B. Allen, in *Quantum Theory of Real Materials*, edited by J. Chelikowsky and S. G. Louie (Kluwer, Dordrecht, in press.)
[28] P. B. Allen, R. M. Wentcovitch, W. W. Schulz, and P. C. Canfield, Phys. Rev. B **48**, 4359 (1993).
[29] A. Kanbayasi, J. Phys. Soc. Jpn. **41**, 1879 (1976).